Dynamics and regulation at the tip : a high resolution view on microtubele assembly

Munteanu, L.

CHAPTER

6 Microtubule catastrophes at molecular resolution

Catastrophes, transitions from growth to shrinkage, are highly regulated in living cells. Information about the molecular events underlying catastrophes are limited to static cryo-EM images of growing and shrinking microtubules and modeling based on mechano-chemical properties of tubulin. Here we used our high-resolution technique to zoom in on catastrophes of dynamic microtubule ends. We observed that fast disassembly events are typically preceded by a slow decrease in microtubule length of several tens of nanometers. We investigated whether this slow decrease is changed when microtubule associated proteins that affect the catastrophe rate, XMAP215 or Mal3, are added.

In cells, microtubule dynamics are highly regulated in order to achieve specific functions at the right time and place. For example high turnover of microtubules at the onset of mitosis allows rapid reorganization of the microtubule array to form the mitotic spindle. How regulatory proteins interfere with the molecular events leading to a catastrophe, is still an open question. This is partly due to the lack of understanding of the molecular mechanism associated with catastrophes. It is well established that the dynamic instability of microtubules is driven by GTP hydrolysis. It was proposed that a stabilizing 'GTP-cap' is required for stable microtubule growth. When this cap is lost the microtubule will transition to rapid depolymerization. Based on cryo-EM micrographs it is believed that the stabilizing cap is represented by a sheet-like structure at the ends of growing microtubules. As shrinking microtubules are characterized by highly curved protofilaments, it is obvious that catastrophes must involve a structural change [39]. It was proposed that closure of the sheet results in a blunt end, corresponding to an intermediate between polymerization and depolymerization [61, 189]. Another idea emerging from cryo-EM studies was that during microtubule elongation, once in a while less stable lattice configurations form at the growing end that could be the origin of catastrophes [190].

In an attempt to shed more light on the molecular events underlying catastrophes, we used our high spatial-resolution technique to follow microtubule growth and shrinkage, and focused on the events right before a fast disassembly event.

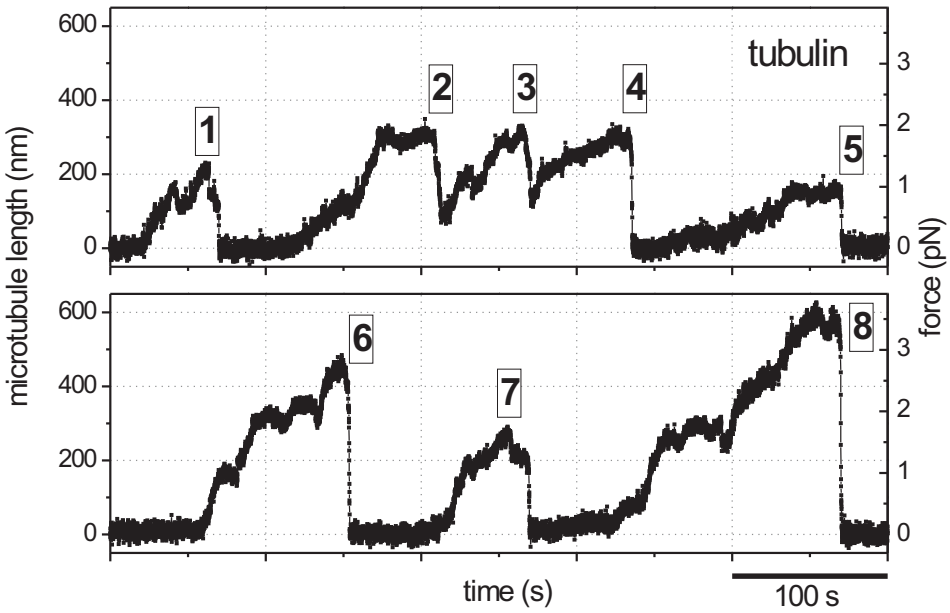

Figure 6.1: Dynamic instability of microtubules measured with optical tweezers. Microtubule length changes (left axis) and the force experienced by the dynamic microtubules (right axis) are plotted. Numbers indicate events with clearly recognizable catastrophes. Microtubules were grown from 5-20 μM tubulin in the absence of MAPs at 25^{o}C. The events presented in the two panels were measured using the same bead-axoneme construct.

6.1 Results

Figure 6.1 shows several growth and shrinking events of individual microtubules, measured with our optical tweezers based technique (chapter 2). Microtubules were grown from axonemes against a rigid barrier. In the trap, microtubules experience a force while growing, indicated on the right axis. A single microtubule growing and shrinking is exemplified by event 5 in figure 6.1. Events 2, 3, and 4 can be explained by the subsequent growth of multiple microtubules, as we do not expect to observe rescues in our experimental conditions. When the first microtubule was shrinking, the bead-axoneme construct moved towards the barrier until another growing microtubule came in contact with the barrier. From that moment on the bead moved again away from the barrier following the growth of the second microtubule. The axonemes used as nucleation centers are nucleating, on average, 1-2 microtubules under our experimental conditions. Even when multiple microtubules were growing from the axoneme, we attributed the shrinking events to single microtubules, as in this situations probably only one microtubule stayed in contact with the barrier.

6.1.1 Is there a molecular signature of catastrophes?

In order to identify a molecular signature of catastrophes, we focused on the events at the onset of fast disassembly events. Figure 6.2 shows individual shrinking events (a and b) for regular tubulin disassembly. For all the events we noticed a common feature: a slow microtubule length decrease prior to a fast disassembly event. Most of the slow length decreases display an approximately constant speed and can take up to several seconds before the microtubule undergoes fast disassembly. There is however a high variability between individual events in the spatial extent of this initial slow length decrease, which ranges from 0 nm to 150 nm (figure 6.2 b). There is also some variability in the total time spanned by the length decrease and in the speeds of the length decrease at short time scale: sometimes the length decrease includes several periods characterized by different depolymerization speeds.

In order to identify microtubule average behavior prior to a fast disassembly event, we aligned the individual segments at the onset of fast shrinkage. The average event is shown in figure 6.2 d. We could identify a reduction in length, which was characterized by a slow speed of 3.1 ± 0.2 $\mu m\ min^{-1}$ (mean $\pm$ s.e.m.) as evaluated by a linear fit over 0.65 s before the onset of the fast disassembly and a length extent of ~ 30 nm. We were wondering if this length decrease was not due to the presence of force against which microtubules were growing. Microtubules experienced, on average, a stall force of 1.4 ± 0.2 pN (mean $\pm$ s.e.m.) (figure 6.2 c). It is possible that under force the bead-axoneme construct constantly rearranges its contact position at the wall, which might appear as a length decrease. To test this option we aligned at a random position pieces of data where the microtubules were stalled and calculated an average event. The average event measured from 14 data stretches showed a flat plateau (figure 6.2 f). Therefore we attribute the decrease in length to molecular events leading to fast shrinkage.

6.1.2 Microtubule catastrophes in the presence of XMAP215 and Mal3

As both XMAP215 (chapter 3) and Mal3 (chapter 5) had clear effects on the catastrophe rate of microtubules, we also investigated whether the two MAPs have a distinguishable effect on the microtubule length evolution just before a fast disassembly event.

Analysis of XMAP215 shrinking events (figure 6.3) revealed a similar length decrease prior to fast disassembly. Figure 6.3 d shows the average event in comparison with the one measured in the absence of XMAP215. The two events are almost identical. However, the individual events in the presence of XMAP215 often display a length decrease prior to fast disassembly that includes several periods of short length decreases, which are characterized by various speeds, together with periods of no length changes. This variability in shape is more often observed with XMAP215 than in the absence of XMAP215, when most of the events prior to fast disassembly are characterized by almost monotonous length decrease. The individual events in the presence of XMAP215 are plotted in figure 6.3 a. We also noticed pauses during the fast periods of shrinkage.

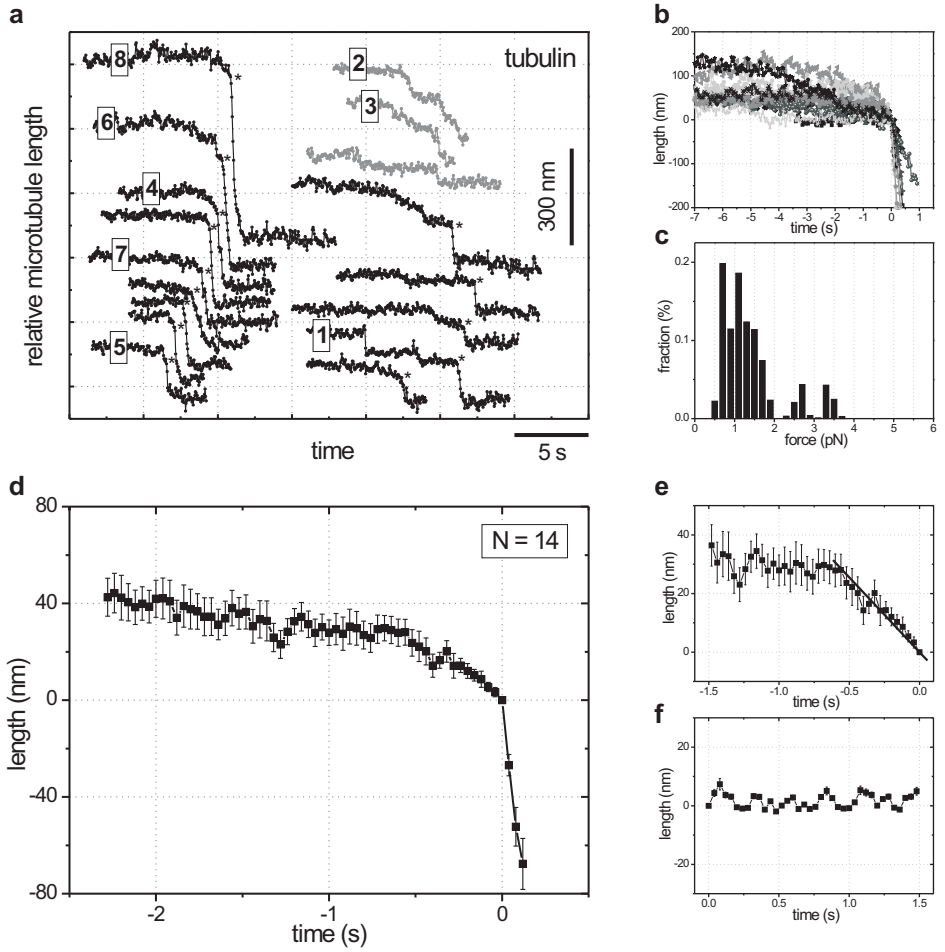

Figure 6.2: Microtubule dynamics before fast depolymerization. **(a)** Individual shrinking events of microtubules assembled in the presence 20 μM tubulin. Numbered traces correspond to the shrinking phases of the events with the same numbers in figure 6.1. The black traces display clear events of fast shrinkage and were aligned at the onset of the fast disassembly phase (indicated by asterisks) with respect to both time and length. The aligned segments are shown in **(b)**, in which the zero's of the coordinate system correspond to the alignment point. In the gray events from **(a)** we did not identify a fast disassembly event. **(c)** Histogram of stall forces including only the plateaus before a complete microtubule depolymerization event. Average stall force experienced by microtubules was 1.4 ± 0.2 pN (mean ± s.e.m.). **(d)** Average behavior of microtubules prior to a fast disassembly phase. The event was determined by averaging the aligned segments from **(b)** (n=14). Error bars represent s.e.m. **(e)** Microtubule length changes during 1.5 seconds just before the fast disassembly phase are compared with **(f)** length changes during 1.5 seconds during the microtubule stall phase. Error bars are s.e.m. The slow reduction in microtubule length before fast disassembly had a speed of 3.1 ± 0.2 μm min^{-1} and it was determined from a linear fit (solid line in **(e)**) over 0.56 s until the onset of fast microtubule disassembly. The error on the speed represents standard error as determined from the linear fit.

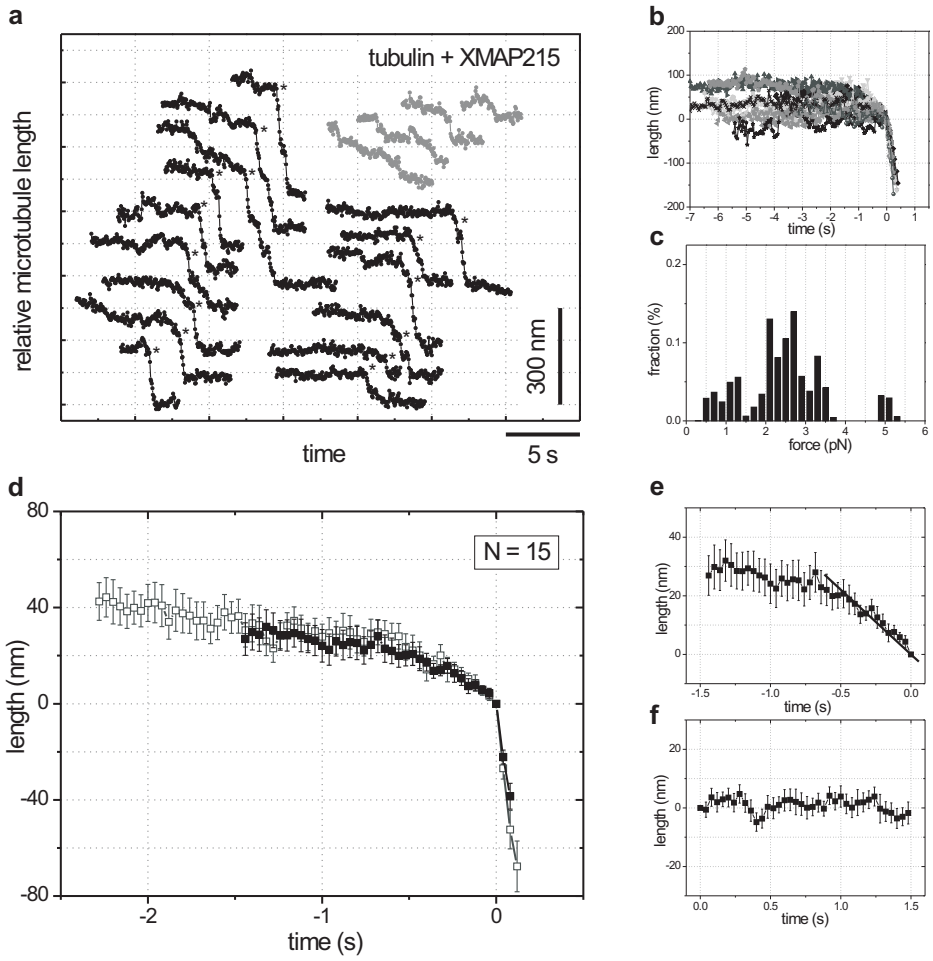

Figure 6.3: Microtubule shrinkage in the presence of XMAP215. **(a)** Individual shrinking events of microtubules assembled in the presence of 20 μM tubulin and 150 nM XMAP215. Black traces display clear events of fast shrinkage and were aligned at the onset of shrinkage (indicated by asterisks). The aligned segments are shown in **(b)**. **(c)** Histogram of stall forces. The average force experienced by microtubules before a catastrophe was 2.4 ± 0.3 pN (mean ± s.e.m.). **(d)** Average event prior to microtubule fast shrinkage in the presence of XMAP215 (solid symbols), determined from the aligned segments (n = 15) shown in **(b)**. The average event evaluated in the absence of XMAP215 (open symbols) (figure 6.2 d) is plotted for comparison. Error bars represent s.e.m. **(e)** Microtubule length changes during 1.5 seconds just before the fast disassembly phase are compared with **(f)** length changes during the microtubule stall phase. Error bars are s.e.m. The slow microtubule length reduction was characterized by a speed of 2.7 ± 0.2 μm min^{-1} as determined from a linear fit (solid line in **(e)**) over 0.56 s until the onset of fast microtubule disassembly. The error on the speed was evaluated from the linear fit.

These pauses resemble the slow length decrease prior to fast disassembly.

In the presence of Mal3 we identified two types of shrinkage events: fast and slow (figure 6.4 a, see also chapter 3). When we averaged the fast events we observed a similar length decrease prior to fast disassembly as in the absence of Mal3 (figure 6.4 d). We also averaged the slow shrinking parts of all events in the following way. The alignment point for the fast ones was the onset of fast disassembly, whereas for the slow ones the alignment point was the end of the slow shrinkage event. The average slow event when all events were included, shown in figure 6.4 d, displays a small up-shift compared with the tubulin or the average fast event. This means that, on average, the length loss through slow depolymerization was more extended in the presence of Mal3 as compared with the absence of the protein. The main contribution comes, however, from the shrinkage events entirely characterized by slow length decrease. The average shrinkage speed of these events is 4.5 ± 0.2 μm min^{-1} (figure 6.4 e), which is higher compared with the one measured for the length decrease prior to fast disassembly in the absence of Mal3.

6.2 Discussion on the mechanism of catastrophes

We can imagine two scenarios for the slow length decrease leading to microtubule fast shrinkage: i) disassembly of a stabilizing sheet-like structure at the microtubule end or ii) stochastic opening of the closed lattice configuration (cylinder) that exists at the end of a stalled microtubule. It is also possible that both scenarios occur sequentially before a fast disassembly event. In the first scenario, the end-structures should survive for up to a minute under force, as we measured stalled microtubules in this time regime prior to the event triggering fast disassembly. In the second scenario, the opening of the cylinder would possibly involve a length extent of several hundred nanometers in order to explain the apparent reduction of 30 nm, given the mechanics of microtubule ends (see section 3.3.1).

XMAP215 does not seem to have an obvious effect on this loss of tubulin dimers or tube opening prior to a fast shrinkage. The pauses during fast period of shrinkage in the presence of XMAP215 might be an indication that XMAP215 is present at the lattice where it has a stabilizing effect: the microtubule can undergo normal fast disassembly, preceded by the slow length decrease, until it encounters an XMAP215 molecule. XMAP215 temporarily prevents the fast disassembly and only when XMAP215 dissociates from the lattice, the microtubule can resume shrinkage.

In the presence of Mal3 we might observe different microtubule structures. The fast events could be interpreted as shrinkage of normal microtubules, that undergo a slow length decrease prior to fast disassembly. This mechanism that triggers microtubule depolymerization seem to be unaffected by the presence of Mal3. The events described entirely by slow shrinkage might represent depolymerization of incomplete microtubules, e.g. sheet-like structures. Mal3 seems to promote formation of such

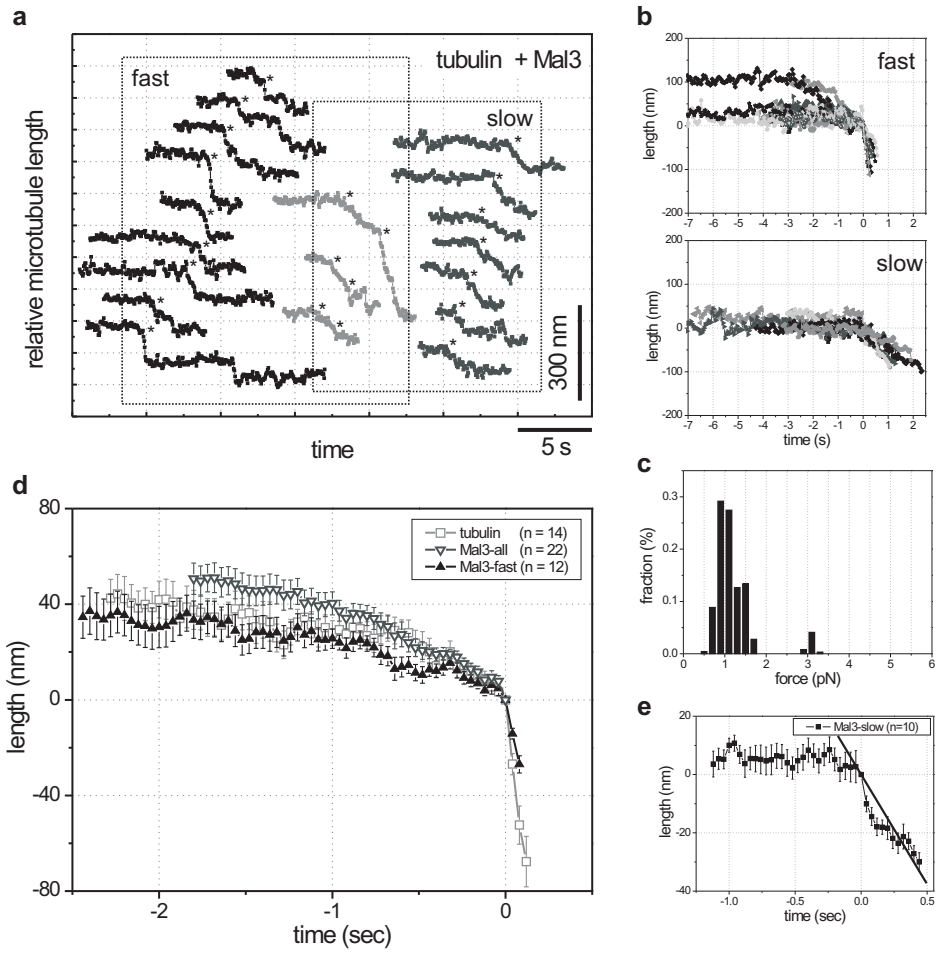

Figure 6.4: Microtubule shrinkage in the presence of Mal3. **(a)** Individual shrinking events of microtubules assembled in the presence of 20 μM tubulin and 200 nM Mal3. Black traces comprise events of fast shrinkage and were aligned at the onset of shrinkage (indicated by asterisks). The aligned segments are shown in **(b)**, top panel. Slow depolymerization events (gray) were aligned approximatively at the beginning of the shrinking phase (asterisks). The aligned slow segments are shown in **(b)**, lower panel. We also identified a couple of events comprising both slow and fast events, shown in light gray in **(a)**. Asterisks indicate the onset of a slow or a fast disassembly phase. **(c)** Histogram of stall forces. The average force experienced by microtubules before a catastrophe was 1.2 ± 0.1 pN (mean ± s.e.m.). **(d)** Averaged events prior to microtubule fast shrinkage in the absence of Mal3 (open squares) (figure 6.2 d) and in the presence of Mal3 are plotted for comparison. Error bars represent s.e.m. The average events in the presence of Mal3 were determined from the aligned fast events (solid triangles) and from all events aligned in such a way that the slow depolymerization part overlapped (alignment point for the fast ones was the beginning of fast shrinkage, whereas the alignment point for the slow events was the end point of the slow shrinkage event) (open triangles). **(e)** Averaged event calculated from the aligned slow events in **(b)**, lower panel. The alignment point was the beginning of the slow depolymerization. Error bars represent s.e.m. The slow depolymerization was characterized by a speed of 4.5 ± 0.2 μm min^{-1} as determined from a linear fit.

structure at the growing microtubule, as we rarely measure shrinkage events fully described by slow depolymerization in the absence of Mal3.

Our observations suggest that catastrophes involve loss of tubulin dimers or a conformational change at the microtubule end. As Mal3 recognizes the growing ends we could probably gain new information on the end-structure under force or prior to a fast disassembly event by monitoring the presence of Mal3 at the end, at the mentioned conditions. Prior *in vivo* experiments suggested that, when microtubules reach the cell cortex, Mal3 signal is lost from the microtubule end some time before shrinkage [109]. We also performed preliminary experiments *in vitro* where microtubules were grown against rigid barriers. The localization of fluorescent Mal3 at the tip was monitored. We observed similar behavior as *in vivo* (data not shown in this thesis). One possible explanation is that first, the end-structure depolymerizes or closes into a tube, hence the disappearing of the Mal3 from the tip, and subsequently, a second event triggers microtubule depolymerization. This event could be the loss of lateral contacts between protofilaments at the tip and might be the slow length decrease observed in our high-resolution measurements. Further experiments on the localization of fluorescent Mal3 at the tip before shrinkage and experiments with other +TIPs that affect the catastrophe rate would be necessary to better understand the molecular events underlying the transition from growth to shrinkage.

Acknowledgements
I thank Tim Noetzel, Kazuhisa Kinoshita and Tony Hyman for kindly providing the XMAP215 protein for us and Linda Sandblad for the kind gift of Mal3 protein.